Angle-resolved photoemission from $Nd_{2-x}Ce_xCuO_4(001)$: A dispersive bandlike Fermi-liquid state of Cu 3*d* character near the Fermi level

Y. Sakisaka, T. Maruyama, and Y. Morikawa
Department of Chemistry, Faculty of Science, Kyoto University, Kyoto 606, Japan

H. Kato
Photon Factory, National Laboratory for High Energy Physics, Tsukuba-shi, Ibaraki 305, Japan

K. Edamoto
Department of Chemistry, Faculty of Science, Tokyo Institute of Technology, Ookayama, Tokyo 152, Japan

M. Okusawa
College of Engineering, University of Osaka Prefecture, Sakai, Osaka 591, Japan

Y. Aiura and H. Yanashima
Institute of Physics, University of Tsukuba, Tsukuba-shi, Ibaraki 305, Japan

T. Terashima and Y. Bando
Institute for Chemical Research, Kyoto University, Uji 611, Japan

K. Iijima, K. Yamamoto, and K. Hirata
Research Institute for Production Development, Kyoto 606, Japan
(Received 8 January 1990; revised manuscript received 14 May 1990)

The electronic structure of $Nd_{2-x}Ce_xCuO_4(001)$ single-crystal thin films, which show (1×1) low-energy electron diffraction patterns, has been studied by angle-resolved ultraviolet photoemission spectroscopy with synchrotron radiation. The data show a well-defined but resolution-limited Fermi edge with a maximum intensity of more than 6% as compared to the main peak intensity. The main peaks exhibit ill-defined dispersion of less than 0.4 eV. All in all, the band calculation can describe the experimental spectra to a fair degree. We find a dispersive bandlike Fermi-liquid state of dominant Cu 3*d* character (almost no O 2*p* and Cu 4*s* character) just below the Fermi level. Its dispersion of 0.2 eV is 8–10 times smaller than that expected from the band calculation. These facts indicate that there is a possibility of Kondo-type renormalized heavy-electron band formation at the Fermi level, caused by spin fluctuations.

I. INTRODUCTION

Recently discovered high-T_c superconductivity in copper oxide[1] has stimulated extensive research in these materials.[2,3] Up to now, all of the high-T_c copper-oxide superconductors have been *p*-type materials with hole carriers, and the formal valence of Cu is more than +2. The holes introduced by doping go into O 2*p* orbitals, so that the states nearest to the Fermi level have mainly O 2*p* character.[4,5] Very recently, Tokura *et al.*[6] have discovered the *n*-type high-T_c superconductor $Nd_{2-x}Ce_xCuO_4$ ($T_c=24$ K at $x=0.15$) with electrons as the charge carriers and the formal Cu valence is less than +2. The extra electrons introduced by Ce^{4+} doping are assumed to enter Cu 3*d* or 4*s* orbitals.[7–9] Hence, the nature of the states at the Fermi level responsible for superconductivity and therefore the electron-pairing mechanism could be different from those in the hole-doped superconductors.

Angle-resolved ultraviolet photoemission spectroscopy (ARUPS) is a useful tool for testing the validity of a band picture in the high-T_c superconductors and for investigating the states near the Fermi level, as shown in the cases of the *p*-type superconductors $YBa_2Cu_3O_{7-x}$ (Ref. 10) and $Bi_2Sr_2CaCu_2O_8$ (Ref. 11). Whether or not a band picture is valid in the normal states above T_c is a vital key factor concerned with the essence of the superconducting mechanism. In the ARUPS studies, dispersive states crossing the Fermi level have been found.[10,11] Such observations seem to point to a conventional bandlike picture in these materials. In other words, despite strong electronic correlations, the high-T_c materials should be viewed as itinerant materials.

In this paper, we present a detailed ARUPS study of high-quality epitaxial $Nd_{2-x}Ce_xCuO_4(001)$ single-crystal thin films at 80 and 300 K to elucidate the normal-state electronic structure.[12] The data show a clear Fermi edge and an occupied-valence-band width comparable to that given by the band calculation of Guo *et al.*[13] The most

important finding is a dispersive bandlike state of dominant Cu $3d$ character just below the Fermi level. Its dispersion of ~ 0.2 eV is $\frac{1}{8}-\frac{1}{10}$ of the calculated value.[13] This band might be related to the Kondo-type resonance state in analogy to the heavy-electron system[14,15] and, if so, it could be concluded that the spin-fluctuation mechanism dominates over the charge-fluctuation one.

II. EXPERIMENT

The ARUPS experiments were mainly done at the Photon Factory as described elsewhere.[10] The electron analyzer has the capacity for independent rotation in the horizontal (rotation angle θ_e along the [100] azimuth) and vertical (rotation angle ϕ_e along the [010] azimuth) planes. The emission angles are denoted by θ_e and ϕ_e. The angular resolution was $\pm 1°$ and the total energy resolution was 0.1–0.2 eV depending on the photon energies ($h\nu$) of 25–90 eV. The pressure in the system was 2×10^{-10} Torr. Throughout the whole experiment, the surface component of the vector potential of the incident linearly polarized synchrotron radiation was in the [100] (ΓX) crystal direction. Data were normalized to the relative flux of incident photons.

The HeI ($h\nu=21.2$ eV) ARUPS spectra were measured using a 127° cylindrical deflector analyzer with an unpolarized He-discharge lamp at Kyoto University. The angular resolution was $\pm 2°$ and the energy resolution was 0.2 eV.

Single-crystal $Nd_{2-x}Ce_xCuO_4(001)$ thin films (10 mm$\times$10 mm$\times$1200 Å, $x\sim 0.17$) with $T_c\sim 12.5$ K were prepared epitaxially on $SrTiO_3(100)$ as described in Ref. 16. The dc resistivity at 300 K was ~ 150 $\mu\Omega$ cm. The sample surfaces were cleaned by heating at 650 °C in $\sim 10^{-6}$ Torr O_2 and subsequently in vacuum (the sample is stable for vacuum heating below ~ 700 °C). The cleanness of the surfaces was checked by Auger electron spectroscopy (AES) and their crystalline order by low-energy electron diffraction (LEED). Small sulfur (S), chlorine (Cl), and carbon (C) AES peaks were detected. Using elemental sensitivity factors, the S, Cl, and C concentration was estimated to be less than 1, 1, and 3 % of the O concentration, respectively. However, we were not able to identify any contribution from these impurities, except for C (see below), to the valence-band ARUPS spectra. The samples showed sharp (1×1) LEED patterns reflecting the square two-dimensional (2D) Brillouin zone (BZ) of the (001) face.

With liquid-N_2 cooling, the samples could be cooled to 80 K. No changes in the AES and ARUPS spectra were recorded over periods of the order of 1–2 d (a half-day was requisite for carrying out a series of ARUPS measurements). However, to make sure, the sample heating to 650 °C in vacuum was repeated every half-day in order to remove possible contamination of residual CO.

A Pt foil in electrical contact with the sample provided the Fermi-level reference of the ARUPS spectra. The work function of the sample was determined to be $\Phi=3.6$ eV by using the secondary electron threshold in photoemission.

III. RESULTS AND DISCUSSION

A. Full valence band

Figure 1 shows the full valence-band photoemission spectra at normal emission from the single-crystal $Nd_{2-x}Ce_xCuO_4(001)$ for $25\le h\nu\le 90$ eV, measured at 300 K. The incidence angle of the radiation is $\theta_i=45°$ from the surface normal. The binding energy is given with respect to the Fermi level (E_F). Eight peaks labeled A–H are seen at ~ 0.2, ~ 1.9, ~ 2.8, ~ 3.6, ~ 5.0, ~ 7.1, ~ 9.7, and ~ 13.8 eV, respectively. Peak C at ~ 2.8 eV is weak but clearly seen in the $h\nu=30$-, 45-, 60-, 70-, and 73-eV spectra. Note that a clear but resolution-limited Fermi-level cutoff is observed.

Peak G at ~ 9.7 eV might be due to a small amount of the residual carbon, for this peak disappeared after the carbon was removed completely by the sample heating to 850 °C in vacuum (however, the dc resistivity of the sample at 300 K increased from ~ 150 to ~ 2000 $\mu\Omega$ cm by this heat treatment, so that the crystal was partially degraded). We found that, in the normal-emission spectra measured after heating to 850 °C (not shown), valence-

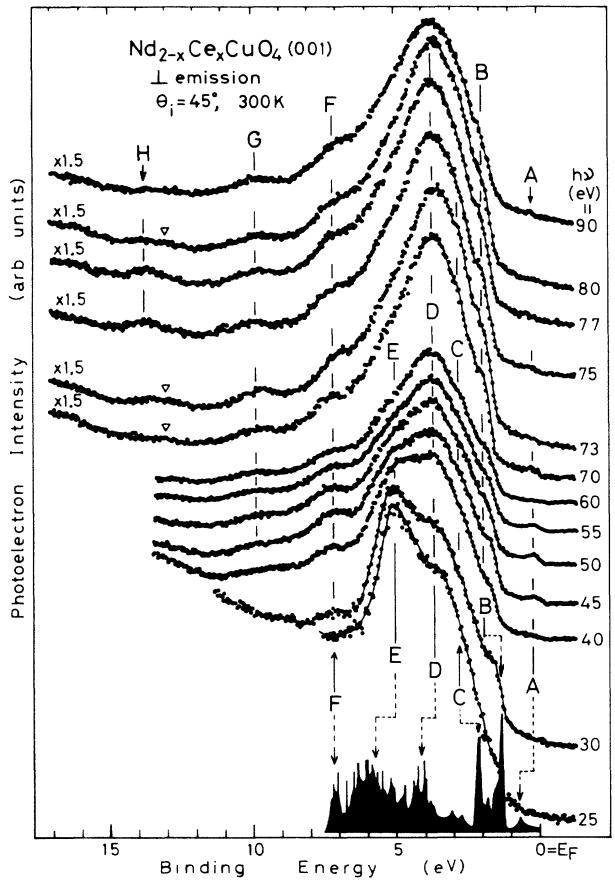

FIG. 1. Valence-band photoemission spectra at normal emission from a single crystal $Nd_{2-x}Ce_xCuO_4(001)$ measured at 300 K and $\theta_i=45°$ for $25\le h\nu\le 90$ eV. Prominent peaks are labeled A–H. At the bottom, the calculated total DOS for $Nd_{1.75}Ce_{0.25}CuO_4$ is shown as a blacked area (from Ref. 13).

band satellite peak H (see below), as well as peak G, disappears and that peak A is remarkably reduced, though the main peaks are nearly unchanged. In principle, a very weak satellite is expected when there is a small charge transfer combined with strong hybridization, so that it needs relatively short time to get the screening charge transferred. We will not discuss the spectra of the degraded samples after heat treatment in detail, for it is unclear what material was produced.

Now, we return to the spectra of the undegraded samples before such heating. Peaks $A-F$ and H are intrinsic to the clean samples. Peaks $A-F$ represent the valence band, which arises primarily from strongly hybridized Cu $3d$ and O $2p$ states.[13] These peaks do not move within ± 0.1 eV with $h\nu$. If these spectra are assumed to be dominated by direct interband transitions (one does not expect that, for the whole range of $h\nu$ between 25 and 90 eV, emission is due to excitation into evanescent gap states), these results indicate the highly two-dimensional nature of the band structure [consistent with a tetragonal crystal structure of this oxide with lattice parameters of $a=3.95$ Å and $c=12.07$ Å (Ref. 6), i.e., $c \gg a$].

For comparative purposes, we show, at the bottom of Fig. 1, the total (summations over all k) density of states (DOS) (dark shading) for $Nd_{1.75}Ce_{0.25}CuO_4$ ($x=0.25$), obtained by the band calculation (Ref. 13). The normal-emission spectra give the k-resolved ($k_{\parallel}=0$) DOS including the optical matrix elements, so that they cannot be directly compared with the total DOS (apart from the different x value). However, peaks $A-F$ can correlate with the gross features in the calculated DOS within ± 0.5 eV as tentatively indicated by dashed lines in Fig. 1 (some peaks A, D, and E are shifted towards the Fermi level, while others B and C are shifted away[17]). Note that the observed valence-band width agrees with the calculated one, though this agreement might be fortuitous because the measured valence bands reflect the excited state where relaxation corrections are important. In addition, emission near the Fermi level is small, in agreement with the calculated DOS. However, we did not observe apparent angular (emission angle dependent) dispersion of more than 0.4 eV for peaks $B-F$, as seen in Fig. 2 where ARUPS spectra measured at $h\nu=40$ eV along $\Gamma \rightarrow M \rightarrow X \rightarrow \Gamma$ are shown (possible dispersion is indicated by solid lines). There, the average position in k space (BZ) where each spectrum probes is also indicated. Such near lack of dispersion could be due to the existence of so many component bands in a narrow energy range.[13] Each peak does not correspond to a single band but to a group of bands. The dispersion effects of different bands could cancel each other in practical ARUPS spectra. The calculation of the k-resolved DOS including the optical matrix elements and the self-energy corrections is desired for the detailed comparison.

As seen in Fig. 1, with increasing $h\nu$ from 25 to 90 eV, peak D becomes monotonically strong relative to peak E, and peak E is scarcely discernible for $h\nu > 70$ eV. According to the calculated atomic photoionization cross-section table,[18] the ratio of the atomic Cu $3d$ and O $2p$ cross sections [σ(Cu $3d$)/σ(O $2p$)] increases with $h\nu$ in this $h\nu$ range. In the 10–60-eV region there are, to our

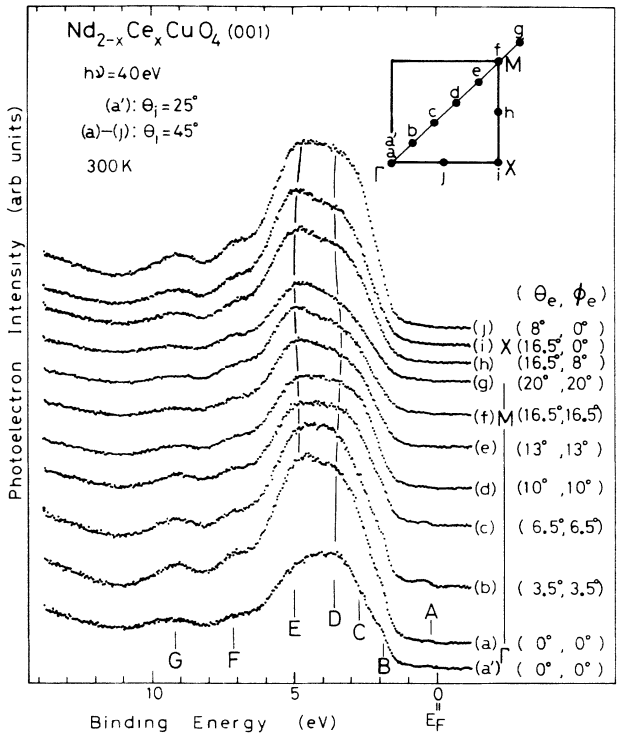

FIG. 2. Angle-resolved photoemission spectra of $Nd_{2-x}Ce_xCuO_4(001)$ along $\Gamma \rightarrow M \rightarrow X \rightarrow \Gamma$ measured at 300 K, $h\nu=40$ eV, and $\theta_i=45°$. The indicated emission angles (θ_e and ϕ_e) are defined by the horizontal (along [100]) and vertical (along [010]) rotation angles of the analyzer. At the bottom, the normal-emission spectrum for $\theta_i=25°$ is also shown [designated as (a')].

knowledge, no experimental σ(Cu $3d$) and σ(O $2p$) data. Although the atomic cross-sectional calculations are not ideal at describing the effects on these heavily hybridized states, it has been shown that, for $YBa_2Cu_3O_{7-x}$, the $h\nu$ dependences of the atomic and solid-state cross sections are nearly identical.[19] The present data suggest that the Cu $3d$ states are more heavily involved in the hybridized bands corresponding to peak D than in those corresponding to peak E.

The 14-eV peak H staying far away from the valence band is observed around $h\nu \sim 75$ eV near the Cu $3p$ resonance, so that it can be ascribed to the well-known valence-band satellite with the two-hole d^8 final-state configuration which is resonantly enhanced on resonance. From comparison of the satellite feature on resonance with those of other copper compounds,[2,10,20] it is found that the position of peak H is just between that of the Cu^{2+} $3d^8$ satellite (~ 13 eV) and that of the Cu^+ $3d^8$ satellite (~ 15 eV). Therefore, we hesitate to decide the Cu valence in $Nd_{2-x}Ce_xCuO_4$, though it has been previously proposed that the Ce doping enhances the population of localized stable Cu^+ (Refs. 7 and 9) or that ~ 0.15 electron per 0.1 Ce atom is donated on all the Cu atoms (Ref. 8). Hence, the effect of Ce doping in $Nd_{2-x}Ce_xCuO_4$ is not simple.

It is remarked that peak H seems to move from ~ 14

eV on resonance to ~13 eV off resonance. In other words, the d^8 valence-band satellite has a resonating higher-binding-energy component at ~14 eV and a nonresonating lower-binding-energy component at ~13 eV (designated by triangles in Fig. 1). The similar shift of the d^8 satellite with $h\nu$ has been previously observed for Ni metal (Ref. 21) and $Pb_2Sr_2PrCu_3O_8$ (Ref. 22). As discussed in detail in Ref. 21, the higher-binding-energy and lower-binding-energy parts are mainly attributed to the ^1G and ^3F multiplets of the d^8 configuration, respectively. The enhancement of the singlet (^1G) satellite on resonance is due to the fact that photoemission from the majority, spin-up band is greatly enhanced relative to that from the minority, spin-down band at the $3p \rightarrow 3d$ resonance, and the singlet-satellite-to-triplet-satellite intensity ratio is estimated to be 1:2 off resonance and 7:3 on resonance (see Ref. 21).

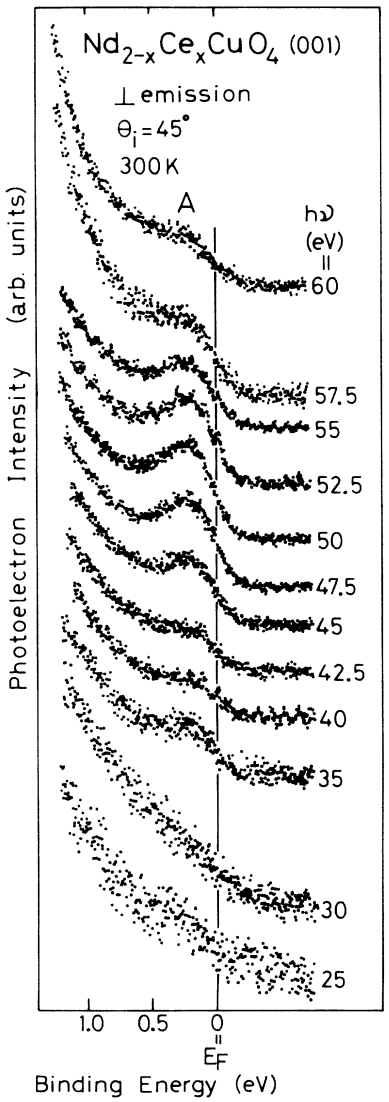

FIG. 3. $h\nu$ dependence of normal-emission spectra of $Nd_{2-x}Ce_xCuO_4(001)$ in the Fermi-edge region measured at 300 K and $\theta_i = 45°$ ($25 \leq h\nu \leq 60$ eV). The spectra were normalized to incident photon flux.

The existence of the satellite and some of the above-mentioned discrepancies between band theory and experiment can be explained to arise from Coulomb correlation effects which are not included in the current single-particle band-structure calculations based on local density theory.[23] The previous studies of the famous valence-band satellite in Ni metal showed that the band model is a reasonable approximation for the ground state and the electron correlations can be treated within perturbation theory.[24-27] Summing up the present results, it can be said that the most of the one-electron models are valid for this oxide, just as they are valid in Ni metal.

B. Fermi-edge region

Figure 3 shows the $h\nu$ dependence of peak A in the normal-emission spectra measured at $\theta_i = 45°$ and 300 K ($25 \leq h\nu \leq 60$ eV). As is more clearly seen in Fig. 4 where the observed peak height is shown (solid circles), peak A is hardly observed for $h\nu < 30$ eV, but it appears at $h\nu \sim 35$ eV and then it is rapidly developed until its maximum intensity is reached at $h\nu \sim 50$ eV, and thereafter it decreases with $h\nu$. That is, peak A exhibits a pronounced intensity maximum at $h\nu \sim 50$ eV. In Fig. 4, the atomic photoionization cross section *per electron* for O

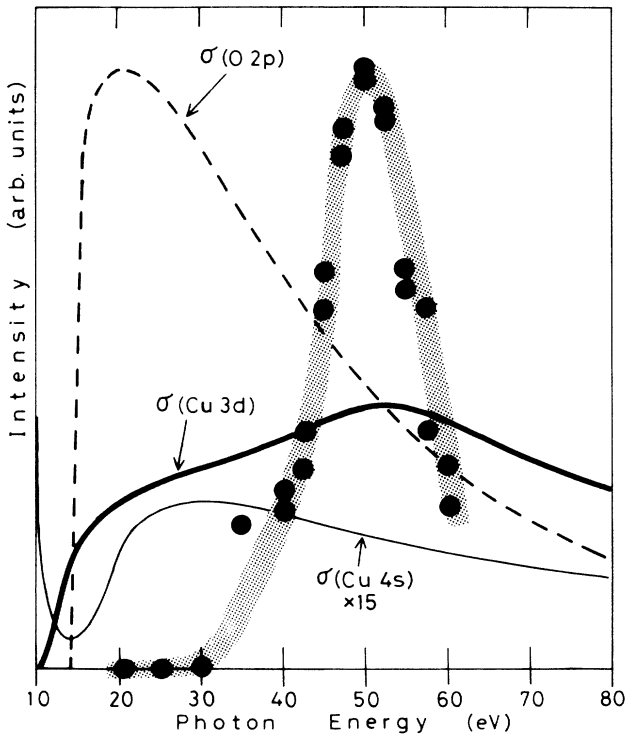

FIG. 4. $h\nu$ dependence of the height of peak A (see the text) just below E_F in the normal-emission spectrum of $Nd_{2-x}Ce_xCuO_4(001)$, plotted by solid circles. The atomic photoionization cross sections *per electron*, σ(O 2*p*), σ(Cu 3*d*), and σ(Cu 4*s*), taken from Ref. 18, are also shown (dashed line, thick solid line, and thin solid line, respectively).

$2p$, Cu $3d$, and Cu $4s$ [σ(O $2p$), σ(Cu $3d$), and σ(Cu $4s$)], taken from Ref. 18, are also shown (dashed line, thick solid line, and thin solid line, respectively) after scaling σ(O $2p$) to the same height of the experimental data. Comparison with σ(O $2p$), σ(Cu $3d$), and σ(Cu $4s$), which peak at $h\nu \sim 20$, 50, and 30 eV, respectively, shows that the electronic state just below the Fermi level has dominant Cu $3d$ character, almost no O $2p$ and Cu $4s$ characters.[28]

Figure 5 shows the normal-emission spectra in the Fermi-edge region measured at $\theta_i = 45°$ and 25° ($h\nu = 50$ eV, 300 K). The intensity of peak A does not show drastic θ_i dependence. Therefore, it can be concluded that peak A of dominant Cu $3d$ character must not have Δ_1 symmetry, but probably Δ_5 symmetry, according to nonrelativistic selection rules for direct transition.[29]

Figures 6 and 7 show the off-normal emission spectra in the Fermi-edge region along $\Gamma \rightarrow X$ and $\Gamma \rightarrow M$, respectively (taken at $h\nu = 50$ eV, $\theta_i = 45°$, and 80 K), revealing a clear dispersion of peak A. The position in k space (BZ) where each spectrum probes is indicated in each figure. Along $\Gamma \rightarrow X$, peak A moves gradually towards higher binding energy by ~ 0.2 eV. Along $\Gamma \rightarrow M$, peak A first shifts towards higher binding energy by ~ 0.2 eV, and then it moves towards the Fermi level by ~ 0.2 eV in the middle between Γ and M, and finally it moves away again from the Fermi level by ~ 0.2 eV.

In order to compare our experimental band structure in the Fermi-edge region with the state-of-the-art band calculation for $Nd_{2-x}Ce_xCuO_4$, in Fig. 8 we plot all the experimental data points [solid circles (●): derived from Figs. 6 and 7; open triangles (△): taken from the unshown spectra] over the calculated band structure of $Nd_{1.75}Ce_{0.25}CuO_4$ ($x = 0.25$) by Guo *et al.* (from Ref. 13). Apparently, there is no simple one-to-one correspondence between experiment and calculation. If the region of bands under consideration is expanded, including the unoccupied bands (though it may lead up to a forced argument), we can find some calculated bands exhibiting larger but qualitatively similar dispersion, e.g., band 1 going from Γ (1.6 eV above E_F) to X (0.7 eV below E_F) and band 2 going from Γ (1.6 eV below E_F) to M (1.6 eV below E_F) via the Fermi level. Band 2 touches the Fermi level in the middle between Γ and M in contrast with the observations. This discrepancy can be attributed to the effect of the instrumental resolution. Note that emission near the Fermi level is largest when the band is actually well below the Fermi level because of the moderate resolution (150 meV). High-resolution data are desired; if it were, the peak would appear much nearer or cross the Fermi level. In any case, what can certainly be said is that the quantitative dispersion of all the calculated bands near the Fermi level is much (~ 10 times) larger

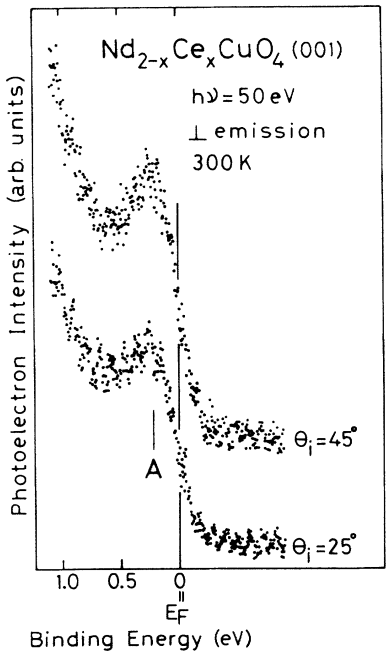

FIG. 5. θ_i-dependent normal-emission spectra of $Nd_{2-x}Ce_xCuO_4$(001) in the Fermi-edge region measured at 300 K and $h\nu = 50$ eV.

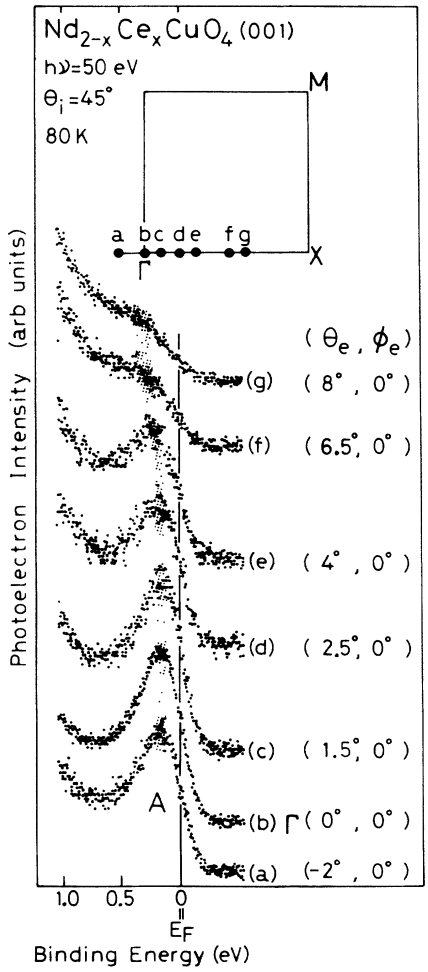

FIG. 6. Angle-resolved photoemission spectra of $Nd_{2-x}Ce_xCuO_4$(001) in the Fermi-edge region along $\Gamma \rightarrow X$ measured at 80 K, $\theta_i = 45°$, and $h\nu = 50$ eV. The indicated emission angles (θ_e and ϕ_e) are defined by the horizontal (along [100]) and vertical (along [010]) rotation angles of the analyzer.

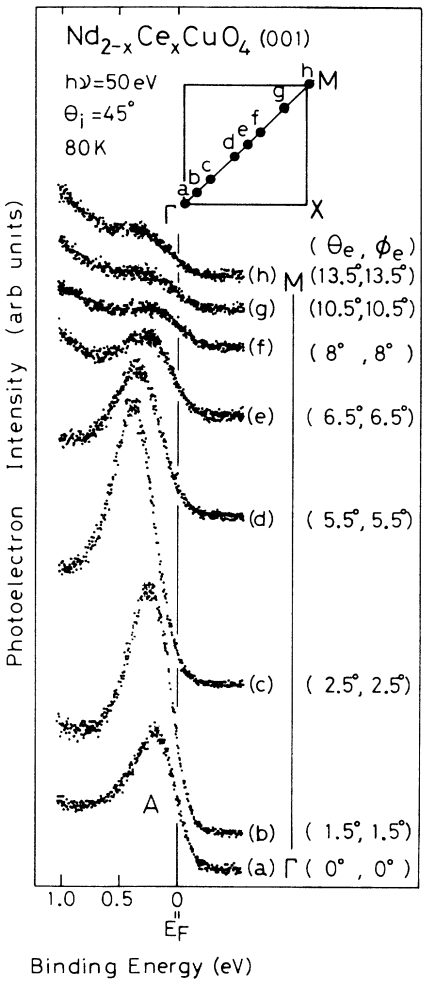

FIG. 7. Angle-resolved photoemission spectra of $Nd_{2-x}Ce_xCuO_4(001)$ in the Fermi-edge region along $\Gamma \rightarrow M$ measured at 80 K, $\theta_i = 45°$, and $h\nu = 50$ eV. The indicated emission angles (θ_e and ϕ_e) are defined by the horizontal (along [100]) and vertical (along [010]) rotation angles of the analyzer.

than that of peak A.

To summarize, a dispersive Fermi-liquid state of dominant Cu $3d$ character exists just below the Fermi level for $Nd_{2-x}Ce_xCuO_4$ in the normal state. Its dispersion is much smaller than predictions of band theory. The formation of the Kondo-type resonance of Cu $3d$ character near the Fermi level (renormalized heavy-electron band formation in analogy to the f-electron systems) has been predicted for high-T_c superconductors with large number of carriers within the normal Fermi-liquid picture.[14,15] Only for $La_{2-x}Sr_xCuO_4$ in the normal state, such a renormalized heavy-electron band structure has been calculated using fitting parameters.[15] This model calculation showed that the quasiparticle DOS (mostly Cu-like) at the Fermi level is strongly enhanced with a mass enhancement of m^*/m between 5 and 8. It has been pointed out that the heavy-fermion picture can readily apply to $Nd_{2-x}Ce_xCuO_4$.[15] Peak A may be related to such a Kondo-type resonance state.

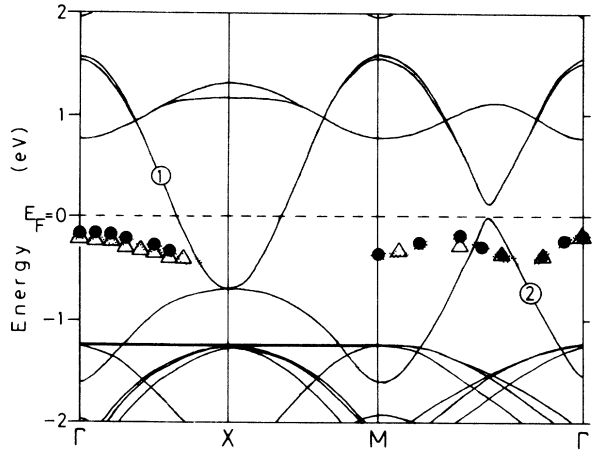

FIG. 8. Binding energies of peak A (see the text) just below E_F as a function of the wave vector $\mathbf{k}$ along Γ-X and Γ-M. The solid circles (●) are data points derived from Figs. 6 and 7, and the open triangles (△) from the unshown spectra. The blowup of the calculated bands for $Nd_{1.75}Ce_{0.25}CuO_4$ near E_F, taken from Ref. 13, is also shown.

IV. CONCLUSION

ARUPS data from $Nd_{2-x}Ce_xCeO_4(001)$ single-crystal thin films reveal a clear Fermi-level cutoff and a dispersive Fermi-liquid state near the Fermi level. In addition, the observed valence-band width agrees with the prediction of band calculation, and a reasonable correspondence of peaks between experiment and calculation is seen, though the main peaks show ill-defined dispersion of less than 0.4 eV. Thus, the single-particle band calculation can describe the ARUPS spectra to a fair degree. In other words, although many-body effects such as a valence-band satellite are observed in the ARUPS spectra, they do not change the fact that such spectra exhibit a clear Fermi edge. Therefore, most of the ARUPS results can be interpreted, in first approximation, within a one-electron theoretical framework, and many-body effects should then be considered in second approximation. In conductors, it seems natural to describe at least the states near the Fermi level by a band picture.

The bandlike Fermi-liquid state just below the Fermi level in $Nd_{2-x}Ce_xCuO_4$ has dominant Cu $3d$ (almost no Cu $4s$ and O $2p$) character, and shows much smaller dispersion ($\sim$0.2 eV) than expected from the band theory. This state may be related to a Kondo-type many-body resonance and an associated renormalized heavy-electron band formed near the Fermi level.[14,15] If so, spin fluctuations must dominate over charge fluctuations.

ACKNOWLEDGMENTS

We are pleased to thank the staff of the Photon Factory, National Laboratory for High Energy Physics, for their excellent support. This work has been performed under the approval of the Photon Factory Program Advisory Committee (Proposal No 89-213).

[1]J. G. Bednorz and K. A. Müller, Z. Phys. B **64**, 189 (1986).
[2]G. Wendin, Phys. Scr. **T27**, 31 (1989), and references therein.
[3]J. Friedel, J. Phys. Condens. Matt. **1**, 7757 (1989), and references therein.
[4]J. A. Yarmoff, D. R. Clarke, W. Drube, U. O. Karlsson, A. Taleb-Ibrahimi, and F. J. Himpsel, Phys. Rev. B **36**, 3967 (1987).
[5]Z.-X. Shen, P. A. P. Lindberg, P. Soukiassian, C. B. Eom, I. Lindau, W. E. Spicer, and T. H. Geballe, Phys. Rev. B **39**, 823 (1989).
[6]Y. Tokura, H. Takagi, and S. Uchida, Nature (London) **337**, 345 (1989).
[7]J. M. Tranquada, S. M. Heald, A. R. Moodenbaugh, G. Liang, and M. Croft, Nature (London) **337**, 720 (1989).
[8]E. E. Alp, S. M. Mini, M. Ramanathan, B. Dabrowski, D. R. Richards, and D. G. Hinks, Phys. Rev. B **40**, 2617 (1989).
[9]G. Liang, J. Chen, M. Croft, K. V. Ramanujachary, M. Greenblatt, and M. Hegde, Phys. Rev. B **40**, 2646 (1989).
[10]Y. Sakisaka, T. Komeda, T. Maruyama, M. Onchi, H. Kato, Y. Aiura, H. Yanashima, T. Terashima, Y. Bando, K. Iijima, K. Yamamoto, and K. Hirata, Phys. Rev. B **39**, 2304 (1989); **39**, 9080 (1989).
[11]C. G. Olson, R. Liu, A.-B. Yang, D. W. Lynch, A. J. Arko, R. S. List, B. W. Veal, Y. C. Chang, P. Z. Jiang, and A. P. Paulikas, Science **245**, 731 (1989).
[12]The preliminary results have already been reported [Y. Sakisaka, T. Maruyama, Y. Morikawa, H. Kato, K. Edamoto, M. Okusawa, Y. Aiura, H. Yanashima, T. Terashima, Y. Bando, K. Iijima, K. Yamamoto, and K. Hirata, Solid State Commun. **74**, 609 (1990)].
[13]G. Y. Guo, Z. Szotek, and W. M. Temmerman, Physica C **162-164**, 1351 (1989).
[14]K. Miyake, T. Matsuura, K. Sano, and Y. Nagaoka, Physica B **148**, 381 (1987).
[15]D. M. Newns, M. Rasolt, and P. C. Pattnaik, Phys. Rev. B **38**, 6513 (1988); D. M. Newns, P. C. Pattnaik, M. Rasolt, and D. A. Papaconstantopoulos, *ibid.* **38**, 7033 (1988); P. C. Pattnaik and D. M. Newns, *ibid.* **41**, 880 (1990).
[16]T. Terashima, Y. Bando, K. Iijima, K. Yamamoto, K. Hirata, K. Hayashi, Y. Matsuda, and S. Komiyama, Appl. Phys. Lett. **56**, 677 (1990).
[17]Similar deviations between theory and experiment have been found for Cu. The calculations of the band structure of Cu based on local density theory place the d bands ~ 0.5 eV too high in energy at some symmetry points and ~ 0.5 eV too low at other symmetry points. See, e.g., R. Courths and S. Hüfner, Phys. Rep. **112**, 53 (1984), Figs. 4 and 5.
[18]J. J. Yeh and I. Lindau, At. Data Nucl. Data Tables **32**, 1 (1985).
[19]J. Redinger, A. J. Freeman, J. Yu, and S. Massidda, Phys. Lett. A **124**, 469 (1987).
[20]M. R. Thuler, R. L. Benbow, and Z. Hurych, Phys. Rev. B **26**, 669 (1982).
[21]Y. Sakisaka, T. Komeda, M. Onchi, H. Kato, S. Masuda, and K. Yagi, Phys. Rev. Lett. **58**, 733 (1987); Phys. Rev. B **36**, 6383 (1987).
[22]D. S. Dessau, Z. X. Shen, P. A. P. Lindberg, B. O. Wells, A. Borg, I. Lindau, W. E. Spicer, J. V. Waszczak, and L. F. Schneemeyer, Phys. Rev. B **40**, 6726 (1989).
[23]Now it is a general consensus that the current local density theory has a deficiency in describing the antiferromagnetic insulating ground states of high-T_c materials, but that there is no objection to band theory for the metallic states.
[24]D. R. Penn, Phys. Rev. Lett. **42**, 921 (1979).
[25]A. Liebsch, Phys. Rev. Lett. **43**, 1431 (1979).
[26]L. C. Davis and L. A. Feldkamp, Solid State Commun. **34**, 141 (1980).
[27]G. Treglia, F. Ducastelle, and D. Spanjaard, J. Phys. (Paris) **43**, 341 (1982).
[28]The reason why the intensity profile of peak A exhibits a sharper peak than σ(Cu $3d$) is not clear but probably due to a superposition of several mechanisms. In the strict sense, the distortion of the valence-electron wave functions in the solid environment with respect to the atomic case should be properly taken into account, though we are dealing with electrons having rather localized nature. Similar atomic-type resonances in photoemission cross section have been observed in the other systems [see, e.g., J. Barth, F. Gerken, and C. Kunz, Phys. Rev. B **31**, 2022 (1985)]. Of course, these transitions can be regarded as band-to-band transitions with huge transition-matrix elements which resemble those for the free atoms at high photon energies. At low photon energies, the solid-state effect becomes predominant.
[29]J. Hermanson, Solid State Commun. **22**, 9 (1979).

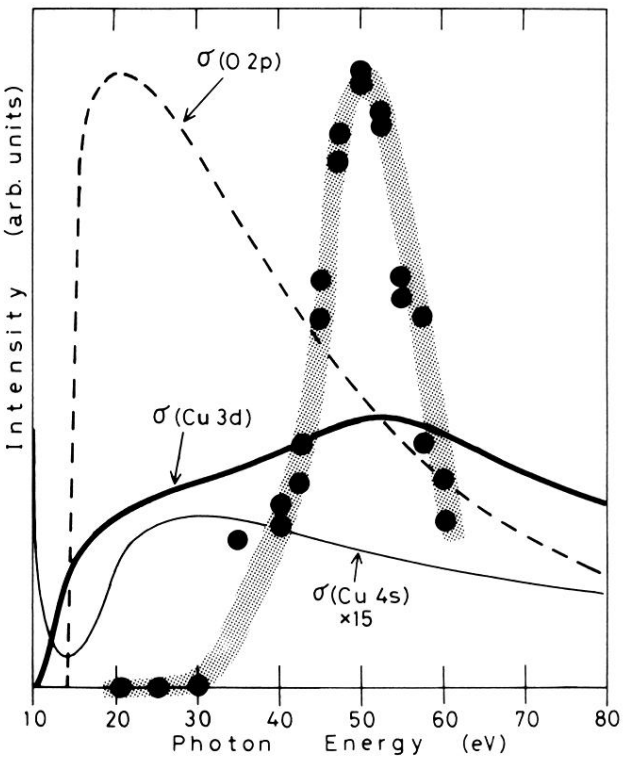

FIG. 4. $h\nu$ dependence of the height of peak A (see the text) just below E_F in the normal-emission spectrum of $Nd_{2-x}Ce_xCuO_4(001)$, plotted by solid circles. The atomic photoionization cross sections *per electron*, σ(O 2*p*), σ(Cu 3*d*), and σ(Cu 4*s*), taken from Ref. 18, are also shown (dashed line, thick solid line, and thin solid line, respectively).

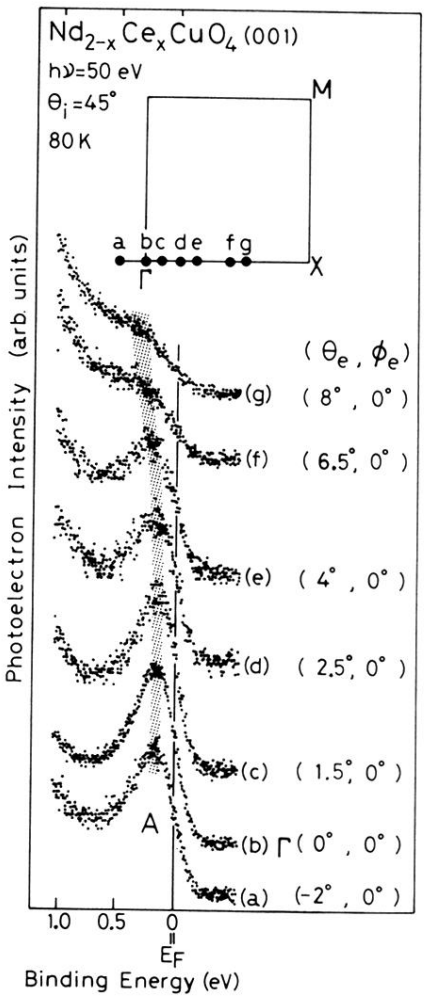

FIG. 6. Angle-resolved photoemission spectra of $Nd_{2-x}Ce_xCuO_4(001)$ in the Fermi-edge region along $\Gamma \rightarrow X$ measured at 80 K, $\theta_i = 45°$, and $h\nu = 50$ eV. The indicated emission angles (θ_e and ϕ_e) are defined by the horizontal (along [100]) and vertical (along [010]) rotation angles of the analyzer.

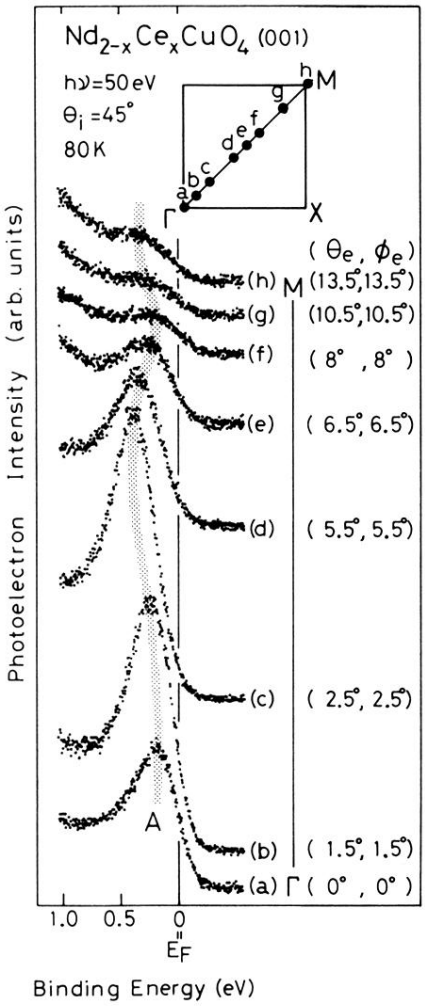

FIG. 7. Angle-resolved photoemission spectra of $Nd_{2-x}Ce_xCuO_4(001)$ in the Fermi-edge region along $\Gamma \rightarrow M$ measured at 80 K, $\theta_i = 45°$, and $h\nu = 50$ eV. The indicated emission angles (θ_e and ϕ_e) are defined by the horizontal (along [100]) and vertical (along [010]) rotation angles of the analyzer.